Glycoconjugate Journal (1996) **13:** 273–283

Negative-ion fast atom bombardment and electrospray ionization tandem mass spectrometry for characterization of sulfated and sialyl Lewis-type glycosphingolipids

TADASHI II[1,2], YOKO OHASHI[1]*, TOMOYA OGAWA[3,4] and YOSHITAKA NAGAI[1]

[1]*Glycobiology Research, Frontier Research Program, The Institute of Physical and Chemical Research (RIKEN), Wako-shi, Saitama 351-01, Japan*
[2]*Research and Development Laboratories, Soda Aromatic Co., Ltd, Noda-shi, Chiba 270-02, Japan*
[3]*Laboratory of Synthetic Cellular Chemistry, The Institute of Physical and Chemical Research (RIKEN), Wako-shi, Saitama 351-01, Japan*
[4]*Faculty of Agriculture, University of Tokyo, Yayoi, Bunkyo-ku, Tokyo 113, Japan*

Received 11 July 1995, revised 13 October 1995

Structural characterization of sulfated and sialyl Lewis (Le)-type glycosphingolipids performed by fast atom bombardment (FAB) and electrospray ionization (ESI) mass spectrometry is described. Both FAB and ESI collision-induced dissociation tandem mass spectrometry (CID-MS/MS) of acidic glycosphingolipids allowed identification of the sulfated or sialyl sugar, and provided information on the saccharide chain sequence. The negative-ion tandem FABMS of sulfated Le-type glycosphingolipids having the non-reducing end trisaccharide ion as the precursor can be used to differentiate the Le^a- and Le^X-type oligosaccharides. The ESI CID-MS/MS of multiple-charged ions provided even more detailed structural information, and some of the useful daughter ions appeared with higher *m/z* values than the precusor because of a lower charge-state. These methodologies can be applied to the structural analyses of glycoconjugates with much larger molecular masses and higher polarity, such as the poly-sulfated and sialyl analogues.

Keywords: sulfated Lewis^a, sulfated Lewis^X, sialyl Lewis^a, sialyl Lewis^X, glycosphingolipid, ESIMS, FABMS, CID-MS/MS

Abbreviations: CID, collision-induced dissociation; ESI, electrospray ionization; FABMS, fast atom bombardment mass spectrometry; Fuc, fucose; Gal, galactose; GlcNAc, *N*-acetylglucosamine; Le, Lewis; Le^a, Lewis^a; Le^X, Lewis^X; MS/MS, mass spectrometry/mass spectrometry; NeuAc, *N*-acetylneuraminic acid; 3-SO_4-Le^a, 3′-sulfated Le^a pentaosyl ceramide; 3-SO_4-Le^X, 3′-sulfated Le^X pentaosyl ceramide; 2,3-SO_4-Le^X, 2′,3′-disulfated Le^x pentaosyl ceramide; 3-S-Le^a, 3′-sialyl Le^a pentaosyl ceramide; 3-S-Le^x, 3′-sialyl Le^X heptaosyl ceramide; 3-S-Le^X-Le^X, 3′-sialyl-Le^x-Le^x octaosyl ceramide.

Introduction

Selectins (namely E-, L- and P-selectins), a family of structurally related cell adhesion proteins have been implicated in adhesive interactions of leucocytes and platelets with cells of the vascular endothelium [1, 2]. Recently, it has been reported that the sulfated Lewis^a (Le^a)- and Lewis^X (Le^X)-determinants are ligands for E-selectin [3], sialyl Le^X and sialyl Le^a for L-selectin as well as E-selectin [4], and acidic Lewis (Le)-type glycoconjugates for the lectin-like molecules on natural killer cells [5]. In order to study the function of these sulfated and sialyl Le-type glycoconjugates at the molecular level and to evaluate therapeutic potentials, it is necessary to

*To whom correspondence should be addressed.

develop efficient and practical methodologies for their structural characterizations.

Ever improving analytical methods have accelerated studies on the nature and biological functions of glycoconjugates and related oligosaccharides in the membrane. Fast atom bombardment mass spectrometry (FABMS) and secondary ion mass spectrometry have proved to be very useful in the analyses of glyconjugates [6] including sulfated and sialyl glycosphingolipids [7, 8]. Recently, we reported that structural characterizations of sulfated tetrasaccharides from glycosaminoglycans were successfully carried out by using both negative-ion FABMS and the collision-induced dissociation tandem mass spectrometry (CID-MS/MS) [9]. Electrospray ionization mass spectrometry (ESIMS) has been shown to be applicable to larger biological samples with high molecular weights [10]. We have reported that ESIMS and MS/MS are useful to characterize acidic glycoconjugates such as polysialogangliosides [11].

Previously, we have shown that both FAB and ESI CID-MS/MS of synthetic sulfated Le^X-type trisaccharides allow identification of the sulfated sugar unit and provide information on the saccharide chain sequence [12]. Here, we describe characterization of synthesized sulfated and sialyl Le-type glycosphingolipids based on the negative-ion FABMS, ESIMS and CID-MS/MS.

Materials and methods

Materials

The compounds examined are shown in Scheme 1. They are 3′-sulfated Le^a pentaosyl ceramide (d18:1/c24:0) (3-SO_4-Le^a) (**1**), 3′-sulfated Le^X pentaosyl ceramide (d18:1/c24:0) (3-SO_4-Le^X) (**2**), 2′,3′-disulfated Le^X pentaosyl ceramide (d18:1/c24:0) (2,3-SO_4-Le^X) (**3**), 3′-sialyl Le^a pentaosyl ceramide (d18:1/c24:0) (3-S-Le^a) (**4**), 3′-sialyl Le^X-Le^x heptaosyl ceramide (d18:1/c24:0) (3-S-Le^X) (**5**) and 3′-sialyl Le^x octaosyl ceramide (d18:1/c24:0) (3-S-Le^X-Le^X) (**6**). All of them were synthesized as the sodium salt [13–15].

Mass spectrometry

Negative-ion FAB mass spectra were recorded on a Finnigan MAT TSQ 700 triple stage quadrupole mass spectrometer equipped with an Ion Tech FAB gun. A xenon beam was used at an energy of 8 keV. About 10 μg of a sample dissolved in 1 μl of a chloroform:methanol mixture (1:1 by vol) was loaded on the FAB target with 1 μl of triethanolamine, which was used as the matrix.

Negative-ion ESI mass spectra were recorded on the Finnigan MAT TSQ 700 triple stage quadrupole mass spectrometer equipped with an electrospray ion source (Analytica of Branford). Samples were typically dissolved in a chloroform:methanol mixture (1:1 by vol) at a concentration of 50 pmol μl^{-1}, and introduced by a mechanical infusion through a microsyringe into the electrospray needle at a flow rate of 1 $\mu l\,min^{-1}$. A potential difference of 3 kV was applied between the electrospray needle and the interior of the ion source, which was kept at the ground potential. Hot nitrogen gas was used to evaporate the solvent from the charged droplets.

CID-MS/MS were taken using a 0.13–0.2 Pa argon as the collision gas at 20–40 eV. At least 10 scans were averaged to obtain each spectrum.

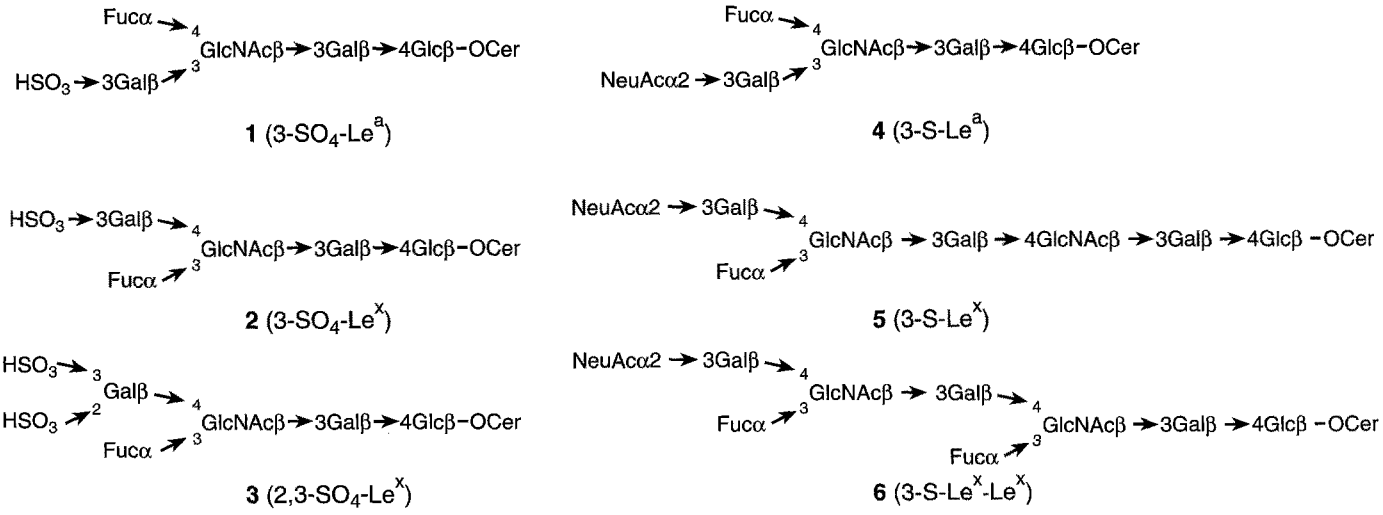

Scheme 1. Structures of compounds examined (**1**–**6**).

Results and discussion

NEGATIVE-ION FAB MASS SPECTRA OF SULFATED AND SIALYL LE-TYPE GLYCOSPHINGOLIPIDS

The negative-ion FAB mass spectra of sulfated Le-type glycosphingolipids (**1–3**) unambiguously gave the molecule-related ions, $[M + (n-1)Na-nH]^-$ (where $n = 1$ for **1** and **2**, $n = 2$ for **3**), as found earlier in similar sulfated saccharide and glycosphingolipids [7, 9, 12]. M represents the relative molecular mass of the free acid as the exact masses throughout this article. The spectra of 3-SO_4-Le^a **1** and 2,3-SO_4-Le^X **3** are shown in Fig. 1a and 1b. In Fig. 1a, predominant molecule-related ions are observed at *m/z* 1564 and 1546, corresponding to the $[M–H]^-$ and $[M–H–H_2O]^-$ ions, respectively. Abundant ions, derived from the cleavages of the glycosidic bonds, were characteristically observed as shown in Scheme 2a. Peaks at *m/z* 1418, 1322, 973, 811 and 649 correspond to the Y-type ions which retain the ceramide moiety. The other type cleavages of the glycosidic bonds yielded some weak peaks corresponding to the B- and C-types ions. The ions, A, B, C, X, Y and Z are referred to by the nomenclature for carbohydrate fragmentation initially proposed by Domon and Costello [16]. Characteristic peaks corresponding to a loss of anhydrofucose (fucose-H_2O) from the $[Y_3\alpha]^-$ and B-type ions individually, are also observed. These results show that the negative charge is not necessarily localized on the sulfated galactose (Gal) of the non-reducing end. Negative-ion FAB mass spectrum of **2**, which is the Le^X-type isomer of **1**, is similar to that of **1** (data not shown). The spectrum of 2,3-SO_4-Le^X **3** shows more complex fragmentation than the case of monosulfated 1 and 2. In Fig. 1b, the molecule-related ions were observed at *m/z* 1666, 1648, 1564, and 1546, corresponding to the $[M + Na–2H]^-$, $[(M + Na–2H)–H_2O]^-$, $[(M + Na–2H)–NaSO_3 + H]^-$ and $[(M + Na–2H)–H_2O–NaSO_3 + H]^-$ ions, respectively. In the negative-ion mode, formation of the ions derived from the loss of 102 amu are observed characteristically for disulfated saccharides, as previously reported [9, 12]. The spectrum of 3 yielded Y-, B- and C-type fragment ions as illustrated in Scheme 2b. In this case, ions derived from the loss of sodium sulfite ($NaSO_3$–H) in addition to the loss of anhydrofucose from $[Y_3\alpha]^-$ and B-type ions are observed. The observations of $[Y_3\alpha]^-$, $[Y_2]^-$, $[Y_1]^-$ and $[Y_0]^-$ ions indicate that the negative charge may not be retained particularly in the disulfated Gal residue of the non-reducing end.

On the other hand, the negative-ion FAB mass spectra of sialyl Le-type glycosphingolipids (**4–6**) exhibited fragmentation features different from those of sulfated analogues. The spectrum of **5** is shown in Fig. 1c as a typical example, and the fragmentation processes are illustrated in Scheme 2c. In Fig. 1c, the intense molecule-related ions are observed at *m/z* 2140 and 2122, corresponding to the $[M–H]^-$ and $[(M–H)–H_2O]^-$ ions. The predominant peaks at *m/z* 1994, 1849, 1687, 1338, 1176, 973, 811 and 649 correspond to the $[Y_5\beta]^-$, $[Y_6\alpha]^-$, $[Y_5\alpha]^-$, $[Y_4]^-$, $[Y_3]^-$, $[Y_2]^-$, $[Y_1]^-$ and $[Y_0]^-$ ions, respectively. The spectrum also shows weak peaks, corresponding to the respective Z-type ions (Fig. 1c and Scheme 2c). Table 1 summarizes molecule-related and major fragment ions in the negative-ion FAB mass spectra of **4–6**. Molecular weight for each compound is clearly shown as peaks, $[M–H]^-$ and $[(M–H)–H_2O]^-$. Although the negative-ion FABMS of gangliosides, *N*-acetylneuraminic acid (NeuAc)-containing glycosphingolipids, yield fragment ions retaining the NeuAc(s) of the non-reducing end [8], the spectra of **4–6** gave another type of fragment ions, which contain the ceramide rather than the NeuAc of the non-reducing end. Characteristic peaks produced either by the elimination of anhydrofucose from the fragment ions containing the fucose (Fuc), or by the cleavages of the glycosidic bonds after the preceding elimination of anhydrofucose from the $[M–H]^-$, are also observed. Table 1 shows fragment ions corresponding to the $[Y_3\alpha]^-$, $[Y_3\alpha–Fuc + H_2O]^-$ and $[Y_2]^-$ ions, and some others for **6**. The observation of $[Y_3\alpha–Fuc + H_2O]^-$, but not of $[Y_2–Fuc + H_2O]^-$ means that there is no Fuc moiety contained in the Y_2-type ion, which supports the anticipated Le^X-Le^X structure for **6**.

NEGATIVE-ION FAB CID-MS/MS SPECTRA OF SULFATED AND SIALYL LE-TYPE GLYCOSPHINGOLIPIDS

(1) Daughter ions from molecule-related ions

The negative-ion CID-MS/MS spectra of sulfated Le-type glycosphingolipids provided different information concerning the structures from those of the normal FABMS. The CID-MS/MS spectra of $[M–H]^-$ of **1** and $[M + Na–2H]^-$ of **3** are shown in Fig. 2a and b, respectively, and their fragmentation processes are illustrated in Scheme 3a and 3b, respectively. In Fig. 2a and b, the B-, C-type ions and the ions corresponding to a loss of anhydrofucose from the B-type ions, all of which contain the sulfated Gal of the non-reducing end, are characteristically observed. These results show that the negative charge is localized on the sulfated Gal of the non-reducing end. The observation of daughter ions with a mass difference of 102 amu between Scheme 3a and b means that the second sulfate group in compound **3** is located in the Gal of the non-reducing end, which is already monosulfated in **1**. No significant difference was observed between the CID-MS/MS of **1** (Fig. 2a) and of the isomer **2** (data not shown), when the $[M–H]^-$ ion of the respective compound was chosen as the precursor ion.

The CID-MS/MS spectrum of $[M–H]^-$ of **4**, as shown in Fig. 2c, indicates the features different from the normal FABMS. An abundant peak at *m/z* 290 and a moderate peak at *m/z* 452 correspond to the $[B_1\alpha–2H]^-$ and $[B_2\alpha–2H]^-$ ions, both containing the NeuAc of the

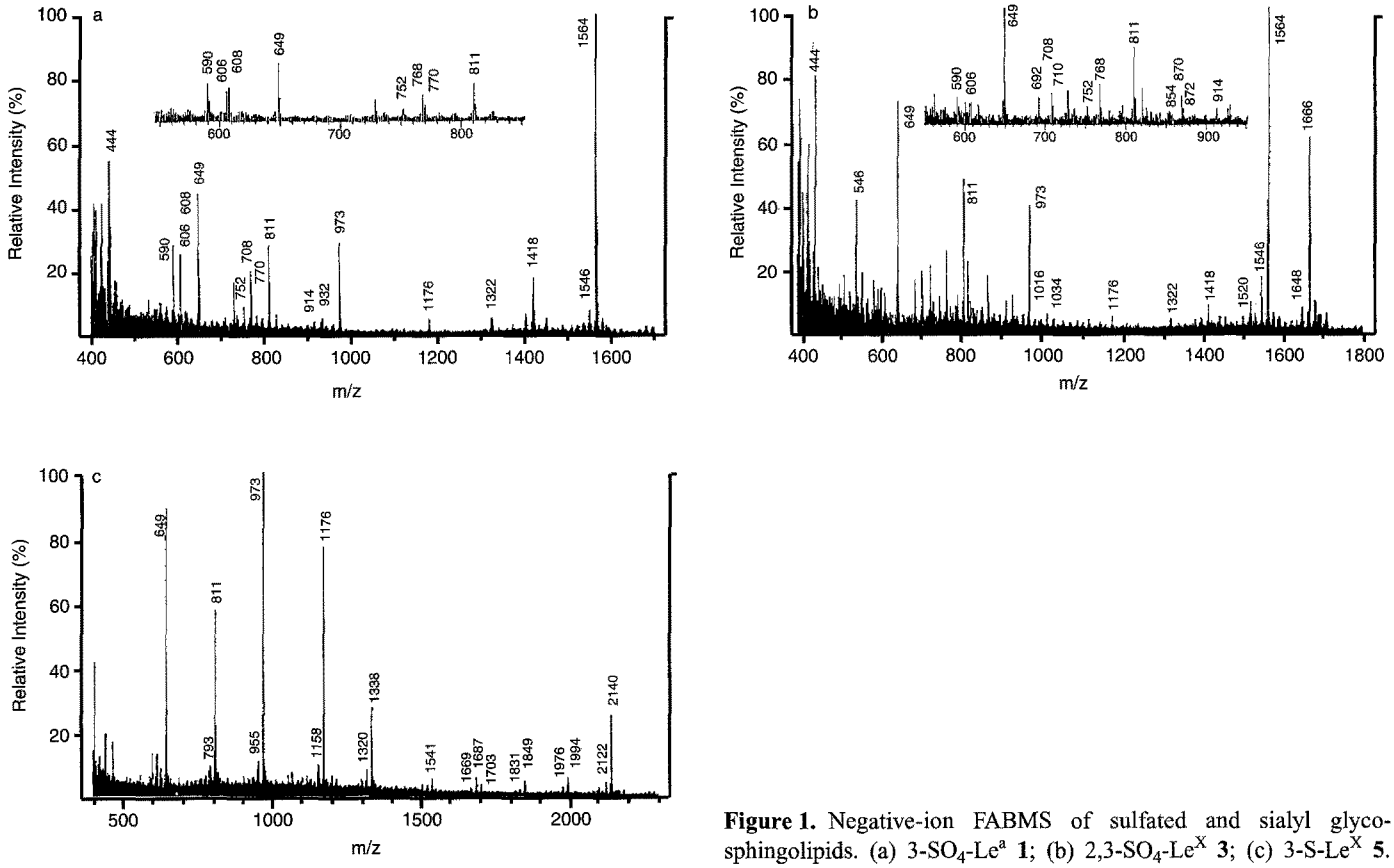

Figure 1. Negative-ion FABMS of sulfated and sialyl glycosphingolipids. (a) 3-SO_4-Le^a **1**; (b) 2,3-SO_4-Le^X **3**; (c) 3-S-Le^X **5**.

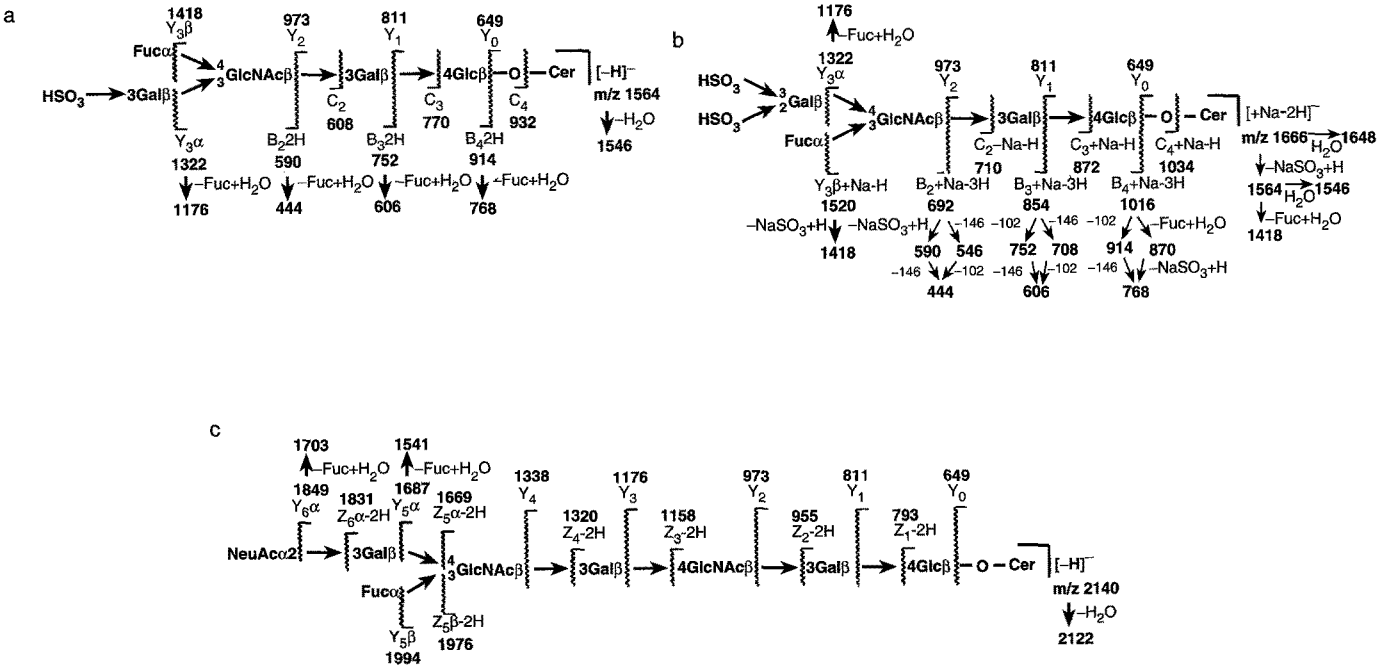

Scheme 2. The fragmentations of the negative-ion FABMS of sulfated and sialyl glycosphingolipids. (a) 3-SO_4-Le^a **1**; (b) 2,3-SO_4-Le^X **3**; (c) 3-S-Le^X **5**.

Table 1. Molecule-related and major fragment ions (*m/z*) in the negative-ion FABMS of sialyl Le-type glycosphingolipids[a].

4	5	6	Ion structure
1775	2140	2286	$[M^b–H]^-$
1757	2122	2268	$[(M–H)–H_2O]^-$
1629	1994	2140	$[(M–H)–Fuc^c + H_2O]^{-d}$
1611	1976	2122	$[(M–H)–Fuc]^{-e}$
	1849	1995	$Y_6\alpha$
	1831	1977	$Z_6\alpha$–2H
	1703	1849	$Y_6\alpha$–Fuc + H_2O
	1687	1833	$Y_5\alpha$
	1669	–[f]	$Z_5\alpha$–2H
	1541	1687	$Y_5\alpha$–Fuc + H_2O
1484	1338	1484	Y_4, $Y_4\alpha$
1466	1320	–	Z_4–2H, $Z_4\alpha$–2H
1338		1338	$Y_4\alpha$–Fuc + H_2O
1322	1176	1322	Y_3, $Y_3\alpha$
1304	1158	1304	Z_3–2H, $Z_3\alpha$–2H
1176		1176	$Y_3\alpha$–Fuc + H_2O
973	973	973	Y_2
955	955	955	Z_2–2H
811	811	811	Y_1
793	793	793	Z_1–2H
649	649	649	Y_0

[a]See Scheme 1 for structures.
[b]M represents the free acid.
[c]Fuc, fucose.
[d]This ion corresponds to $[Y_3\beta]^-$ (for **4**) and $[Y_5\beta]^-$ (for **5** and **6**) ions, respectively.
[e]This ion corresponds to $[Z_3\beta–2H]^-$ (for **4**) and $[Z_5\beta–2H]^-$ (for **5** and **6**) ions, respectively.
[f]Intensities (–) are below 2%.

non-reducing end. Other peaks at *m/z* 1629 1484, 1322, 973, 811 and 649 are assigned to the $[Y_3\beta]^-$, $[Y_4\alpha]^-$, $[Y_3\alpha]^-$, $[Y_2]^-$, $[Y_1]^-$ and $[Y_0]^-$ ions, respectively, as illustrated in Scheme 3c.

(2) Daughter ions from the $[C_2]^-$-type fragment ions

As mentioned above, the negative-ion FABMS of sulfated Le-type glycosphingolipids produced the $[C_2]^-$-type fragment ions containing the trisaccharides of the non-reducing end. The two structurally isomeric monosulfated **1** and **2**, and disulfated **3** were studied by CID-MS/MS having the fragment ions that correspond to the respective $[C_2]^-$-type ions as the precursor ions. The spectra of **1** and **2** provided sufficient information to distinguish the isomers, in contrast to the CID-MS/MS of the molecule-related ions. The CID-MS/MS of **1** and **2** of the respective fragment ion at *m/z* 608, which corresponds to the $[C_2]^-$ ion, are shown in Fig. 3a and b. The spectrum of **1** (Fig. 3a) exhibits the diagnostic peaks at *m/z* 462, 259 and 241, corresponding to the $[Y_{1'}\beta]^-$, $[C_1\alpha]^-$ and $[B_1\alpha–2H]^-$ ions, respectively, where $Y_{1'}\beta$ is the daughter ion that corresponds to the $Y_1\beta$ fragment of the trisaccharide precursor ion (*m/z* 608) and whose structure is shown in Scheme 4a. On the other hand, the spectrum of **2** (Fig. 3b) shows a characteristic peak at *m/z* 444, corresponding to the $[Z_{1'}\beta–2H]^-$ ion in addition to the $[Y_{1'}\beta]^-$, $[C_1\alpha]^-$ and $[B_1\alpha–2H]^-$ ions (Scheme 4b). These results show that the Fuc molecule linked at the C-3 position of GlcNAc is more easily eliminated as a neutral molecule than that linked at the C-4. This phenomenon of the cleavage of 3-*O*-glycoside of the non-reducing end site in GlcNAc is congruent with the earlier finding in negative-ion FABMS of underivatized branched oligosaccharides [17].

The above-stated fragmentation rules were applicable to **3**. As shown in Fig. 3c, the CID-MS/MS of **3** having the $[C_2 + Na–H]^-$ ion (*m/z* 710) as the precursor ion characteristically gave the $[Y_{1'}\beta + Na–H]^-$, $[Z_{1'}\beta + Na–3H]^-$, $[C_1\alpha + Na–H]^-$ and $[B_1\alpha + Na–3H]^-$ ions (Scheme 4c). These observations indicate that distinction of sulfated Le^a- from Le^X-type glycosphingolipids can be implemented by negative-ion FAB CID-MS/MS having the $[C_2]^-$-type ions as the precursors.

The above-stated fragmentation rule does not apply, however, to sialyl Le-type glycosphingolipids, because the less acidic carboxylate group fails to retain the negative charge at the non-reducing end. Therefore, the key ion corresponding to $[C_3]^-$-type ion does not appear in the normal FABMS of **4–6**.

NEGATIVE-ION ESI MASS SPECTRA OF SULFATED AND SIALYL LE-TYPE GLYCOSPHINGOLIPIDS

The negative-ion ESI mass spectra of sulfated and sialyl Le-type glycosphingolipids **1–6** clearly exhibited the single-charged and double-charged ions. The negative-ion ESIMS of 2,3-SO_4-Le^X **3**, for which two negative charges are readily generated by dissociation of the two sulfates, as shown in Fig. 4b, sensitively showed peaks at *m/z* 1666 and 821.5 corresponding to the $[M'–Na]^-$ ion and the double-charged ion $[M'–2Na]^{2-}$. M′ represents the full sodium salt. However, the spectra of **1**, **2** and **4–6**, which have only one acidic functional group such as sulfate or carboxylate, showed complex adduct ions with doubly charged-state, as reported previously for neutral glycosphingolipids [18]. The ESI mass spectra of **1** and **4** are shown in Fig. 4a and c. Table 2 summarizes molecule-related ions observed in the negative-ion ESI mass spectra of **1–6**. In the high mass region in Fig. 4a, two peaks at *m/z* 1564 and 1586 corresponding to the $[M'–Na]^-$ and $[M'–H]^-$ ions are observed. Three predominant peaks at *m/z* 781.5, 799.5 and 826.5 correspond to unusual adduct ions $[M–Na–H]^{2-}$, $[M–Na + Cl]^{2-}$ and $[M–Na + 89]^{2-}$, respectively.

The negative-ion ESIMS of **4** with a NeuAc, gave the usual single-charged ions, and unusual double-charged ions as obtained in the monosulfated **1** and **2**. In Fig. 4c, peaks at *m/z* 1775 and 1797 correspond to the $[M'–Na]^-$

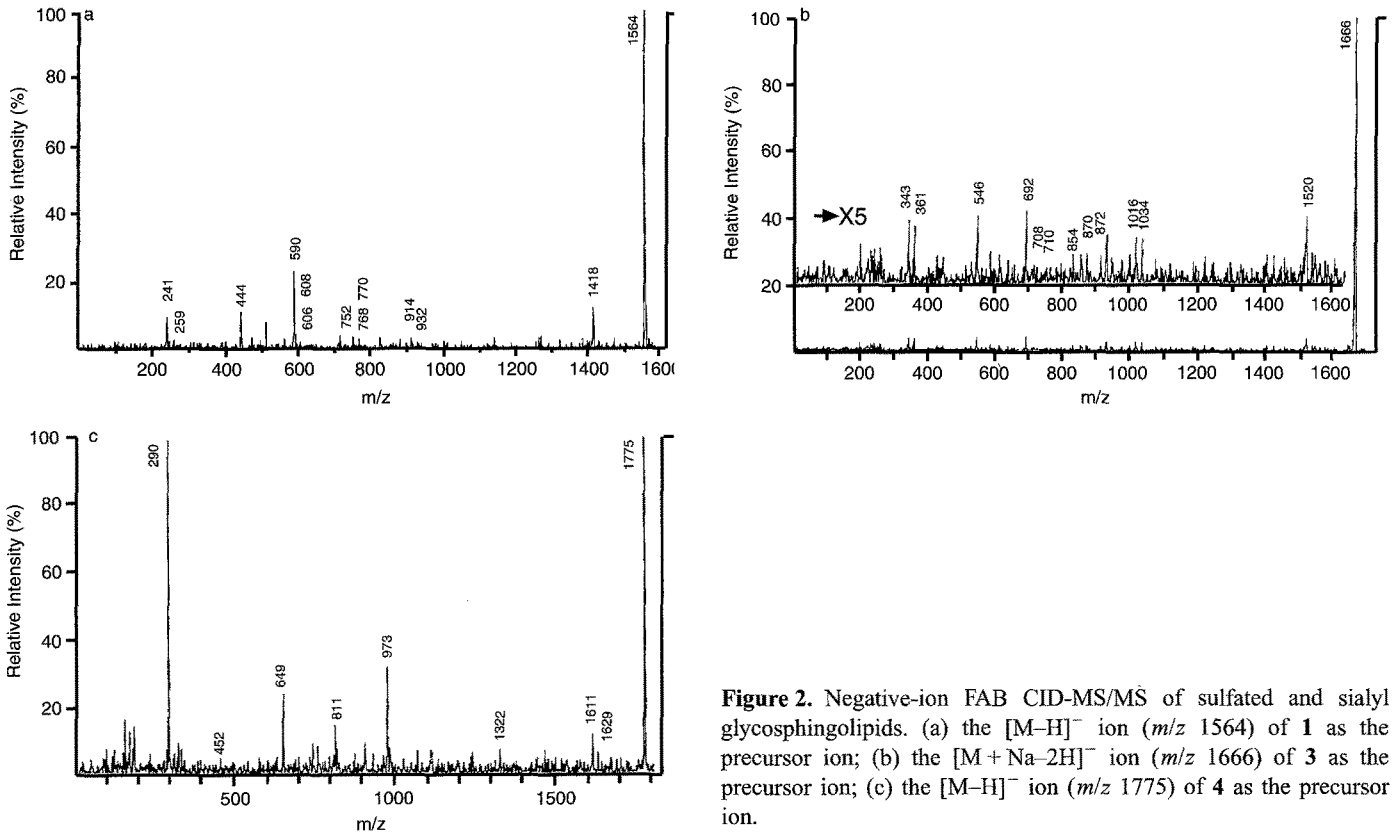

Figure 2. Negative-ion FAB CID-MS/MS of sulfated and sialyl glycosphingolipids. (a) the $[M–H]^-$ ion (*m/z* 1564) of **1** as the precursor ion; (b) the $[M + Na–2H]^-$ ion (*m/z* 1666) of **3** as the precursor ion; (c) the $[M–H]^-$ ion (*m/z* 1775) of **4** as the precursor ion.

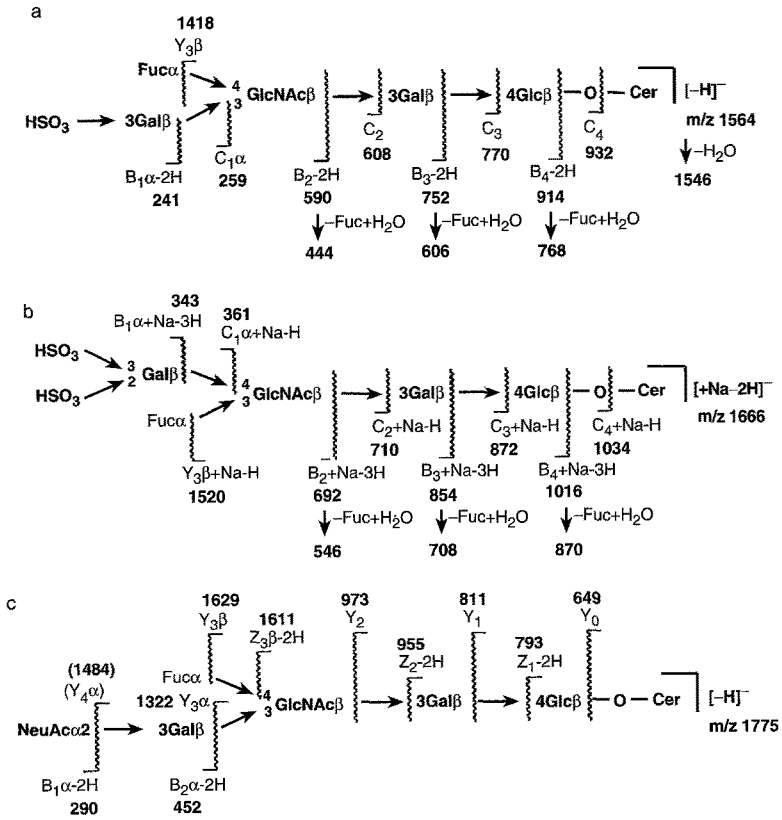

Scheme 3. The fragmentations of the negative-ion FAB CID-MS/MS of sulfated and sialyl glycosphingolipids. (a) the $[M–H]^-$ ion (*m/z* 1564) of **1** as the precursor ion; (b) the $[M + Na–2H]^-$ ion (*m/z* 1666) of **3** as the precursor ion; (c) the $[M–H]^-$ ion (*m/z* 1775) of **4** as the precursor ion.

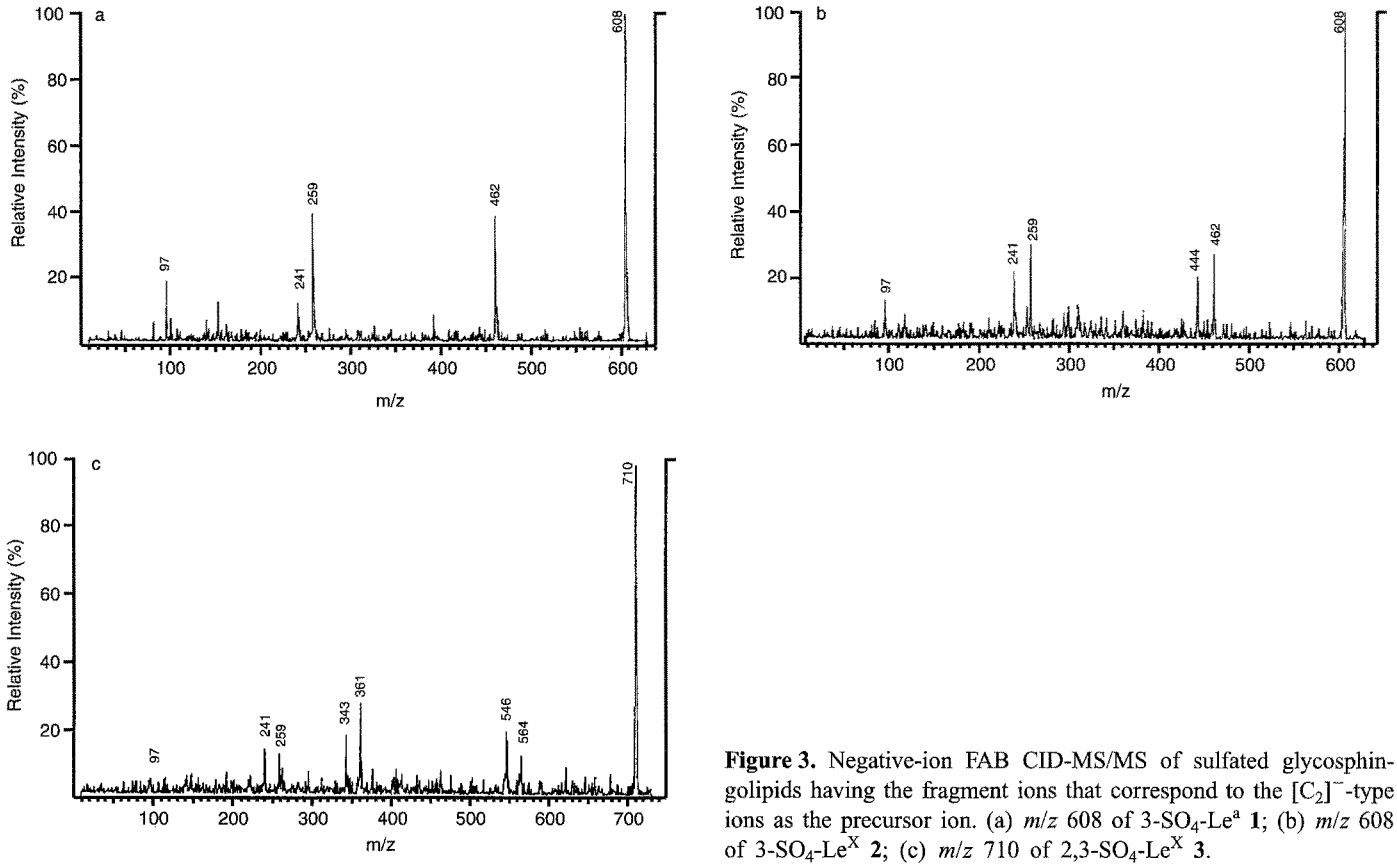

Figure 3. Negative-ion FAB CID-MS/MS of sulfated glycosphingolipids having the fragment ions that correspond to the $[C_2]^-$-type ions as the precursor ion. (a) *m/z* 608 of 3-SO_4-Le^a **1**; (b) *m/z* 608 of 3-SO_4-Le^X **2**; (c) *m/z* 710 of 2,3-SO_4-Le^X **3**.

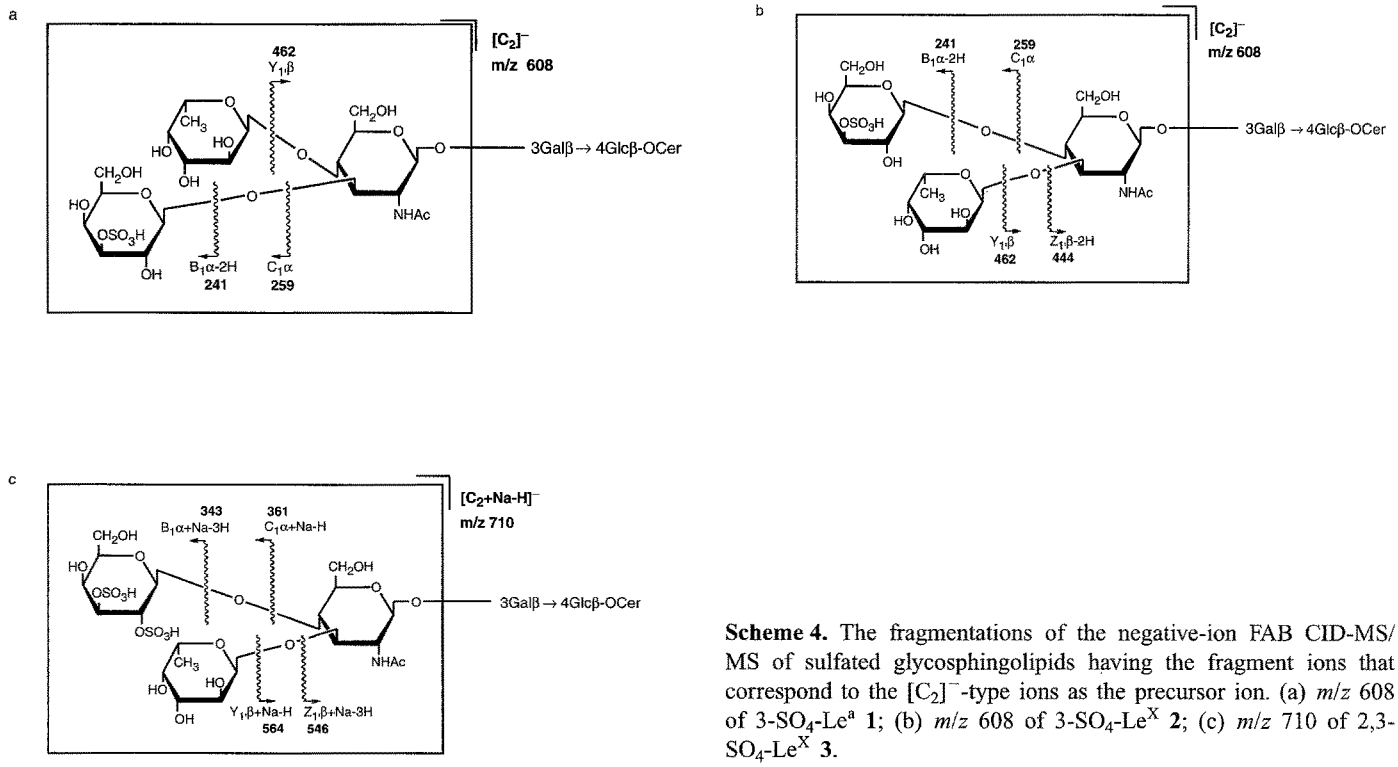

Scheme 4. The fragmentations of the negative-ion FAB CID-MS/MS of sulfated glycosphingolipids having the fragment ions that correspond to the $[C_2]^-$-type ions as the precursor ion. (a) *m/z* 608 of 3-SO_4-Le^a **1**; (b) *m/z* 608 of 3-SO_4-Le^X **2**; (c) *m/z* 710 of 2,3-SO_4-Le^X **3**.

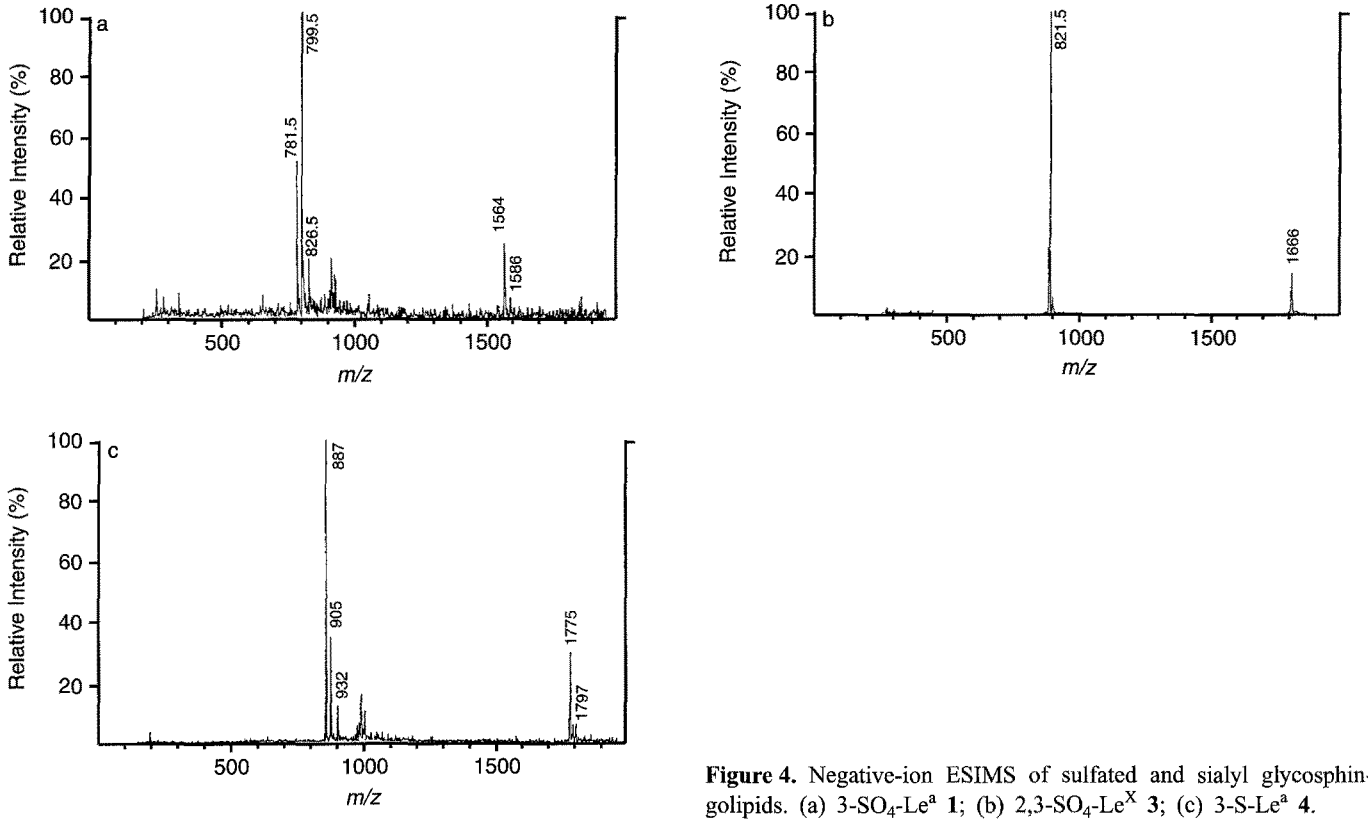

Figure 4. Negative-ion ESIMS of sulfated and sialyl glycosphingolipids. (a) 3-SO_4-Le^a **1**; (b) 2,3-SO_4-Le^X **3**; (c) 3-S-Le^a **4**.

Table 2. Results of the negative-ion ESIMS of sulfated and sialyl Le-type glycosphinoglipids.

Compound[a]	M'[b]	Observed ions *m/z* (relative intensity %)					
		Single-charged ion		Double-charged ion			
		$[M'-H]^-$	$[M'-Na]^-$	$[M'-Na+89]^{2-}$	$[M'-Na+Cl]^{2-}$	$[M'-Na-H]^{2-}$	$[M'-2Na]^{2-}$
1	1587	1586 (6)	1564 (22)	826.5 (17)	799.5 (100)	781.5 (77)	
2	1587	1586 (5)	1564 (52)	826.5 (12)	799.5 (26)	781.5 (100)	
3	1689	–[c]	1666 (14)	–	–	–	821.5 (100)
4	1798	1797 (7)	1775 (31)	932 (13)	905 (35)	887 (100)	
5	2163	–	2140 (55)	–	1087.5 (14)	1069.5 (100)	
6	2309	–	–	1187.5 (19)	1160.5 (100)	1142.5 (43)	

[a]See Scheme 1 for structures.
[b]M' represents the full sodium salt.
[c]Intensities (–) are below 2%.

and $[M'-H]^-$, and abundant ions at *m/z* 887, 905 and 932 correspond to the $[M'-Na-H]^{2-}$, $[M'-Na+Cl]^{2-}$ and $[M'-Na+89]^{2-}$ ions, respectively. These observations suggested that the Cl^-- and $C_4H_9O_2^-$-adduct ions are produced not only from neutral glycosphingolipids but also from acidic glycosphingolipids which have a dissociable acidic functional group such as carboxylate or sulfate. These results showed that in the negative-ion mode, the maximum charge-state of observed multiply-charged ions may not correspond solely to the number of acidic functional groups, but also depend on the size of the sugar chains of glycosphingolipids. There are cases in which the maximum charge-state is larger than the number of acidic functional groups, because of the addition of negative species such as Cl^- or $C_4H_9O_2^-$. In the negative-ion ESIMS, the solvent mixture of methanol and chloroform, which is widely used to dissolve the glycosphingolipids, produces complex adduct ions with multiple-charges, but these adduct ions give useful information on the molecular masses.

NEGATIVE-ION ESI CID-MS/MS SPECTRA OF SULFATED AND SIALYL LE-TYPE GLYCOSPHINGOLIPIDS

(1) Daughter ions from single-charged precursor ions

The result of ESI CID-MS/MS of the single-charged ion $[M + Na–2H]^-$ ($[M'–Na]'$) of 2.3-SO_4-Le^X **3**, as shown in Fig. 5a, is similar to that of FAB CID-MS/MS (Fig. 2b), except for the peaks in the lower mass region. Spectral features observed in the lower mass region from *m/z* 90 to 500 (Fig. 5a) are similar to those observed in the negative-ion FAB CID-MS/MS of disulfated Le^X trisaccharide, as previously reported for sulfated trisaccharides [12]. The presence of these ions shows that the structure of **3** contains the partial structure of disulfated Le^X trisaccharide, which has the disulfated Gal at the non-reducing end. Spectral features of ESI CID-MS/MS having the single-charged ion $[M–H]^-$ ($[M'–Na]^-$) of **4** as the precursor, as shown in Fig. 5b, are much like the above-described FAB CID-MS/MS (Fig. 2c) of the same sample.

These results may indicate that the $[M–H]^-$ and $[M + Na–2H]^-$ ($[M'–Na]^-$) ions produced by ESIMS have internal energies and ion structures similar to the $[M–H]^-$ and $[M + Na–2H]^-$ ($[M'–Na]^-$) ions produced by FABMS.

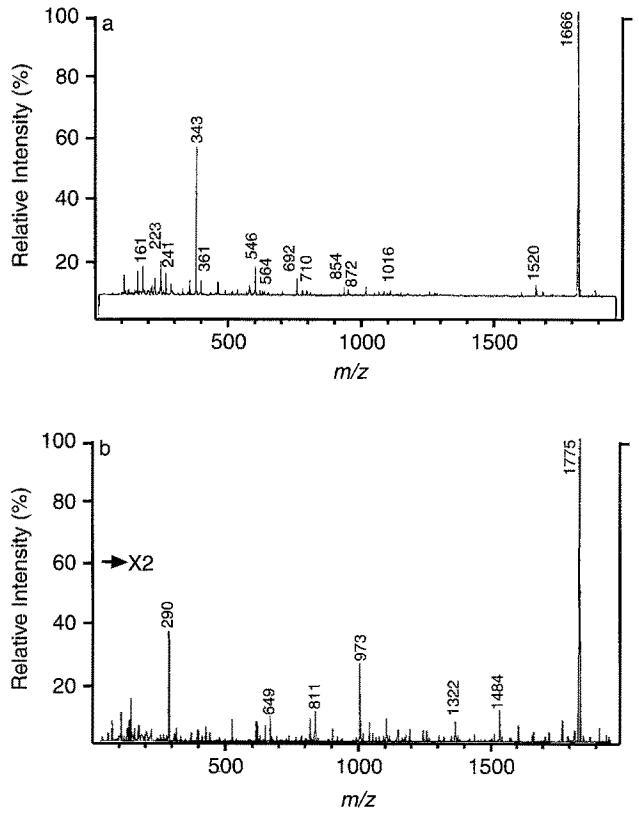

Figure 5. Negative-ion ESI CID-MS/MS of sulfated and sialyl glycosphingolipids. (a) the $[M + Na–2H]^-$ ion (*m/z* 1666) of **3** as the precursor ion; (b) the $[M–H]^-$ ion (*m/z* 1775) of **4** as the precursor ion.

(2) Daughter ions from double-charged precursor ions

The CID-MS/MS of the double-charged ion $[M'–2Na]^{2-}$ provided much information on the characteristics of the structure. The spectrum of **3** having the $[M–2H]^{2-}$ ($[M'–2Na]^{2-}$) ion at *m/z* 821.5, as shown in Fig. 6a, gave a series of double-charged ions at *m/z* 160 ($[B_1\alpha–3H]^{2-}$), 334.5 ($[B_2–3H]^{2-}$), 415.5 ($[B_3–3H]^{2-}$), 496.5 ($[B_4–3H]^{2-}$) and 748 ($[Y_3\beta–H]^{2-}$) produced by the cleavages of the glycosidic bonds. C-type ions were not detected as double-charged. Peaks at *m/z* 1546 and 1400 correspond to the ions derived by the eliminations of $[HSO_4]^-$ from the precursor ion, and by the additional loss of anhydrofucose from the ion at *m/z* 1546, respectively. Other peaks are assigned as the single-charged ion produced by the elimination of SO_3 with the intra-molecular proton transfer, as illustrated in Scheme 5a. A characteristic of the single-charged daughter ions from the double-charged ion $[M'–2Na]^{2-}$ is that most of the C-type ions are more abundant than the B-type ions; *i.e.* $[C_4]^-$ (*m/z* 932) > $[B_4–2H]^-$ (*m/z* 914), $[C_3]^-$ (*m/z* 770) > $[B_3–2H]^-$ (*m/z* 752), $[C_2]^-$ (*m/z* 608) > $[B_2–2H]^-$ (*m/z* 590). The origin of the peak at *m/z* 392 is not yet clear. These results indicate that the double-charged ion $[M'–2H]^{2-}$ of **3**, produced by ESIMS, may have two negative charges on the disulfated Gal of the non-reducing end.

As a typical example of CID-MS/MS of sialyl Le-type glycosphingolipids having the double-charged ion as the precursor, the spectrum of **4** having $[M–2H]^{2-}$ ($[M'–Na–H]^{2-}$) ion (*m/z* 887) as the precursor is shown in Fig. 6b. In contrast to the normal FABMS and CID-MS/MS of the single-charged ion $[M–H]^-$, the peaks are observed at *m/z* 290 ($[B_1\alpha–2H]^-$), 470 ($[C_2\alpha]^-$), 819 ($[C_3]^-$) and 981 ($[C_4]^-$), all of which retain the NeuAc of the non-reducing end. Other peaks at *m/z* 649, 973 and 1466 correspond to the $[Y_0]^-$, $[Y_2]^-$ and $[Z_4\alpha–2H]^-$, respectively (Scheme 5b). This result indicates that the double-charged ion $[M–2H]^{2-}$ ($[M'–Na–H]^{2-}$) of **4**, produced by ESIMS, may have two negative charges, one on the NeuAc of the non-reducing end and another on the ceramide moiety, as reported previously for the ESI CID-MS/MS of gangliosides [11].

These observations show that the CID-MS/MS of double-charged ions as the precursor provides structural information for the sugar sequences, and some of the useful daughter ions appeared with higher *m/z* values than the precursor because of a lower charge-state [11].

Conclusion

Negative-ion FAB mass spectra of sulfated and sialyl Le-type glycosphingolipids show the fragment ions derived from the cleavages of glycosidic bonds, as well as distinct

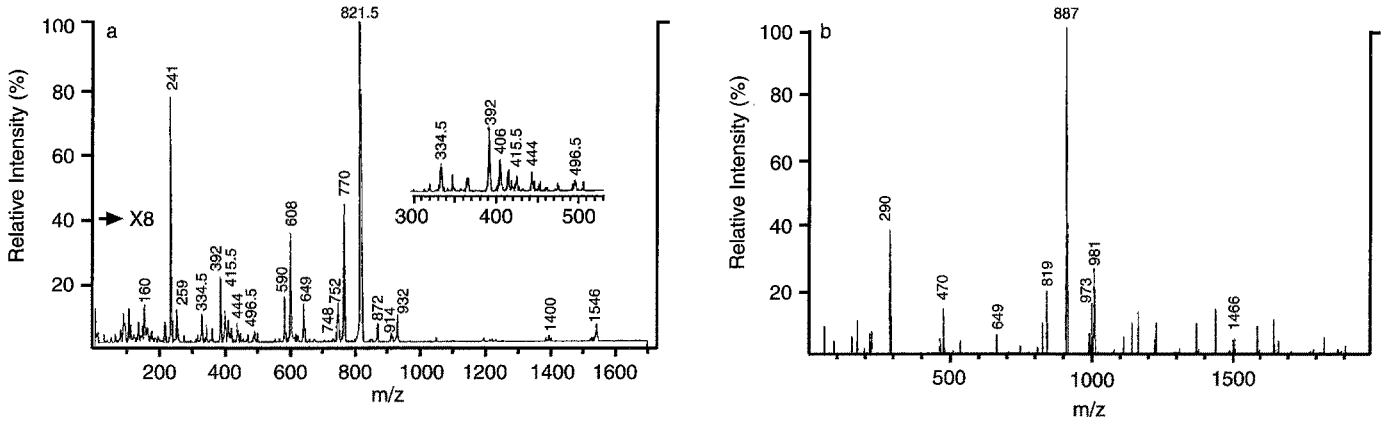

Figure 6. Negative-ion ESI CID-MS/MS having double-charged ions as the precursor ions. (a) the $[M–2H]^{2-}$ ($[M'–2Na]^{2-}$) ion (*m/z* 821.5) of **3**; (b) the $[M–2H]^{2-}$ ($[M'–Na–H]^{2-}$ ion (*m/z* 887) of **4**.

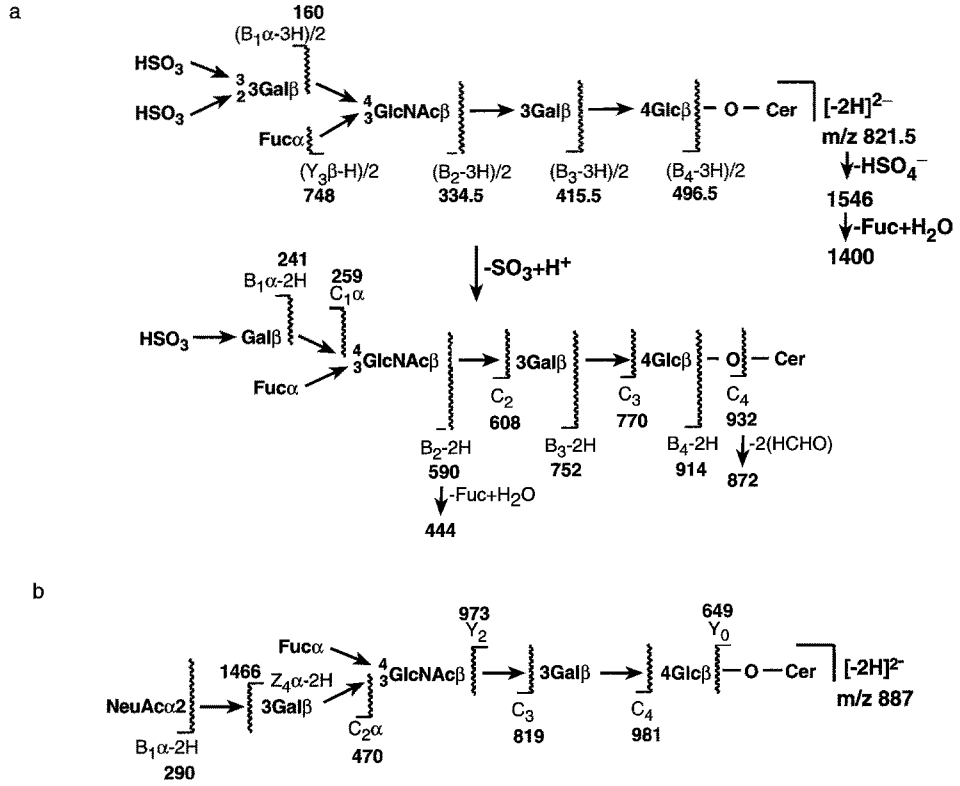

Scheme 5. The fragmentations of the negative-ion ESI CID-MS/MS having double-charged ions as the precursor ions. (a) the $[M–2H]^{2-}$ ($[M'–2Na]^{2-}$) ion (*m/z* 821.5) of **3**; (b) the $[M–2H]^{2-}$ ($[M'–Na–H]^{2-}$) ion (*m/z* 887) of **4**.

molecule-related ions. The CID-MS/MS of the selected molecule-related ions provides useful structural information, including location of the sugar unit which contains acidic functional group(s). The most important finding in the present study is that the negative-ion tandem FABMS of sulfated Le-type glycolipids specifying the non-reducing end trisaccharide ion as the precursor can be used to distinguish Le^a- from Le^X-type isomers.

The negative-ion ESI mass spectra clearly exhibited the single-charged and double-charged ions. An interesting phenomenon in ESIMS of these acidic glycosphingolipids is that the second charge to produce a double-charged ion is gained by an extra deprotonation or an attachment of a novel ion such as Cl^- or $C_4H_9O_2^-$. The ESI CID-MS/MS of double-charged ions as the precursor provides structural information for the sugar sequences, and some of the useful daughter ions appeared with higher *m/z* values than the precursor because of a lower charge-state.

These results suggest that the negative-ion tandem FAB or ESIMS will provide a new rapid and convenient method for the analysis of sulfated or sialyl glycosphingolipids. These findings will be applied to the structural elucidations of various glyconjugates with much larger molecular masses and highly polar functional groups, such as sulfates or carboxylates.

Acknowledgements

The authors thank Dr Shigeki Nunomura, Mr Masami Iida and Mr Masaaki Numata of Nissin Food Products Corporation for their kind gifts of synthesized samples. We are thankful to our colleague Dr Sadamu Kurono, without whose effort in maintaining the instrument in the best condition, we could not have carried out the present study. This work was partially supported by the Grant-in-Aid for Scientific Research on Priority Areas No. 06240247 from the Ministry of Education, Science and Culture, Japan.

References

1. Watson SR, Fennie C, Lasky LA (1991) *Nature* **349**: 164–67.
2. Lasky LA (1992) *Science* **258**: 964–69.
3. Yuen C-T, Lawson AM, Chai W, Larkin M, Stoll MS, Stuart AC, Sullivan FX, Ahern TJ, Feizi T (1992) *Biochemistry* **31**: 9126–31.
4. Berg EL, Magnani J, Warnock RA, Robinson MK, Butcher EC (1992) *Biochem Biophys Res Comm* **184**: 1048–55.
5. Bezouska K, Yuen C-T, O'Brien J, Childs RA, Chai W, Lawson AM, Drbal K, Fiserova A, Pospisil M, Feizi T (1994) *Nature* **372**: 150–57.
6. Peter-Katalinic J (1994) *Mass Spectrom Rev* **13**: 77–98.
7. Tadano-Aritomi K, Kasama T, Handa S, Ishizuka I (1992) *Eur J Biochem* **209**: 305–13.
8. Kasama T, Handa S (1991) *Biochemistry* **30**: 5621–24.
9. Ii T, Kubota M, Hirano T, Ohashi M, Yoshida K, Suzuki S (1995) *Glycoconjugate J* **12**: 282–89.
10. Smith RD, Loo JA, Bushman M, Udseth HR (1991) *Mass Spectrom Rev* **10**: 359–452.
11. Ii T, Ohashi Y, Nagai Y (1995) *Carbohydr Res* **273**: 27–40.
12. Ii T, Ohashi Y, Nunomura S, Ogawa T, Nagai Y (1995) *J Biochem (Tokyo)* **118**: 526–33.
13. Endo A, Iida M, Fujita S, Numata M, Sugimoto M, Nunomura S (1995) *Carbohydr Res* **270**: C9–C13.
14. Nunomura S, Iida M, Mumata M, Sugimoto M, Ogawa T (1994) *Carbohydr Res* **263**: C1–C6.
15. Iida M, Endo A, Fujita S, Numata M, Matsuzaki Y, Sugimoto M, Nunomura S, Ogawa T (1995) *Carbohydr Res* **270**: C15–C19.
16. Domon B, Costello CE (1988) *Glycoconjugate J* **5**: 397–409.
17. Garozzo D, Impallomeni G, Montaudo G, Spina E (1992) *Rapid Commun Mass Spectrom* **6**: 550–52.
18. Ii T, Ohashi Y, Nagai Y (1993) *Org Mass Spectrom* **28**: 927–28.